Hindawi
Advances in Polymer Technology
Volume 2023, Article ID 9313467, 12 pages
https://doi.org/10.1155/2023/9313467

Research Article

Fused Deposition Modeling of Single-Use Plastic Alloy

Wang Liao, Jie Wang, and Manping Pan

School of Science, Xihua University, Chengdu 610039, China

Correspondence should be addressed to Wang Liao; liaowang@mail.xhu.edu.cn

Received 24 October 2022; Revised 6 January 2023; Accepted 12 January 2023; Published 14 February 2023

Academic Editor: Kinga Pielichowska

Packaging plastics are called 'single-use plastics' because of short lifetime. Among which, the three plastics of polyethylene (PE), polypropylene (PP), and polyethylene terephthalate (PET) take more than 70%. Due to incompatibility, few research has been done on the alloy of the three plastics. The aim of this study is to investigate the possibility of single-use plastic alloy (SUPA) of ternary PE, PP, and PET as the 3D printing material. Tensile and bending tests are carried out to investigate the mechanical properties, photographs of scanning electron microscope (SEM) are taken for morphology analysis, and differential scanning calorimetry (DSC) are used to study the crystallization behavior of the alloys. The results show that there is an optimal ratio for all the components to obtain the best mechanical performances, i.e., the ratio of PP/PE = 40/60 with 20 wt% PET, 2 wt% maleic anhydride grafted polypropylene (PP-g-MAH) and 2 wt% organic modified montmorillonite (OMMT). This SUPA has a tensile strength of 14.48 MPa, a tensile modulus of 586.42 MPa, a flexural strength of 15.85 MPa, and a flexural modulus of 544.67 MPa. Due to the function of compatibilizer and nanoclay (NC) will be affected by redundancy, the potential primary fibrosis while collecting the feeding filaments and the secondary fibrosis at the nozzle of 3D printing might be responsible for the variation of the mechanical performances.

1. Introduction

A huge number of plastics and waste plastics (WPs) are expected to be continuously produced [1]. Among all the plastics, packaging has the largest output of ca. 40%. The most important polymers used for packaging plastics are polyethylene (PE), polypropylene (PP), and polyethylene terephthalate (PET), which take more than 70% [2]. They are discarded after being used once and therefore are called 'single-use plastics' [3, 4]. As a result, the single-use plastics become the most abundant municipal waste in many countries. Although recycling methods for plastics continue to appear [5–7], highly mixed state is still the biggest obstacle for WPs management. Processing of highly mixed WP blends without classification will lead to recycled products with deteriorated properties and appearances. Furthermore, plastic mixtures without being sorted out cannot be depolymerized and repolymerized to new materials.

For the single-use plastics, both PE and PP are polyolefins (POs). Despite constituent and structural similarities, it has been well established that PE and PP are highly immiscible in the whole range of composition, which results in poor mechanical properties [8]. The research of PO blends can be traced back to the 1960s [9]. At the beginning of this century, due to the recycling pressure of the huge amounts of POs and establishment of new processing methods, the research on PO blends were further deepened with respect to the micromorphology and crystallization behavior [10–13]. Recently, the predictions of the theoretical models have agreed well with the experimental results in terms of Young's modulus and impact strength of PO blends [14]. On the other hand, the polymer chain of PET is essentially different from those of POs for its full of polar groups. PO/PET blend is therefore with poor interfacial adhesion and two-phase morphology [15, 16]. Although various compatibilizers [17, 18] and new processing methods are used, microfibrillar reinforced composite [19, 20], for instance, are developed; a valuable route for PE/PET or PP/PET blend recovery has not been satisfactorily established.

Plastics are not necessarily disordered or downgraded after mixing. In fact, plastic alloy is a promising design to improve the overall performances of mixed plastics [21–23], in which

one component is compatible well with the other one. In addition, nanoclays (NCs) are widely used to fabricate polymer composites [24]. If the surfaces of NCs are compatible with the polymer, incorporation of the NCs could hence effectively reinforce the (mixed) plastics [25]. At present stage, alloys with two polymers are well studied [15, 26, 27]. However, alloy with components more than that number has been rarely reported. There may be 3 main restricts for this situation: (i) the complexity of the research system, (ii) lack of suitable research object, and (iii) lack of suitable research method.

Additive manufacturing (AM), or 3D printing, enables people to reduce consumption of raw material and customize required products [28, 29]. Currently, two types of AM technologies are prevalent in industry, i.e., selective laser sintering [30] and fused deposition modeling (FDM) [31, 32]. FDM is the most common method for polymers. In which, a feeding filament is drawn out of a heated extrusion head and immediately deposit onto a bed in a layer-by-layer way to form the required part [33–35]. At present, acrylonitrile-butadiene-styrene plastic, polylactic acid, polyamide, polystyrene, and polycarbonate are commonly adopted as the raw materials. However, large-scale application of FDM is still constrained due to the cost and insufficient performance. To the best of our knowledge, research on mixed plastics as the raw material for AM is still limited, let alone the mixed plastics with more than 2 components.

The aim of this study is to investigate the possibility of single-use plastic alloy (SUPA) of ternary PE, PP, and PET as the FDM feeding material. The ratio of each component is based on its proportion in actual production. The processing conditions, the content ratio of the plastics, the effect of a compatibilizer, and a typical NC will be discussed. We hope the results of this study could give an initial momentum to value-added utilization of complex WPs.

2. Experimental Section

2.1. Materials. All the plastics (PE, PP, and PET) were purchased from Sinopec Co. and were dried in an oven at 70°C for 12 h before use. Maleic anhydride-grafted polypropylene (PP-g-MAH) and sodium montmorillonite (MMT) were purchased from Shanghai Aladdin Biochemical Technology Co., Ltd. 1-Cetylpyridine chloride was purchased from Shanghai Energy Chemical, Co., Ltd. Organic modified montmorillonite (OMMT) was obtained by adding 50 mL 1-cetylpyridine chloride aqueous solution (0.094 mol/L) into 150 mL MMT dispersion (26.7 g/L) at 80°C and stirring for 8 h. The obtained OMMT was washed thoroughly by water and ethanol and then dried at 80°C.

2.2. Preparation of Filaments. The required amounts of raw materials were weighed and mixed manually before added into the micro twin-screw extruder (WLG10AG, Shanghai Xinshuo Precision Machinery Co., Ltd.). The processing temperature started from 245°C, and the screw speed was set at 25 r/min. The resulting filaments were drawn out at a constant speed of 20 cm/min to produce even filament ($d = 1.75$ mm). The filament was dried at 70°C for 12 h before it was fed to the 3D printer (JG MAKER A5S, Shenzhen Aurora Technology Co., Ltd.). The parameters for 3D printing are layer height of 0.1 mm, filling density of 100 wt%, nozzle temperature of 230°C, platform temperature of 30°C, and printing speed of 60 mm/s. The formulas of all the tested specimens are listed in Table 1.

2.3. Mechanical Tests and Characterizations. The specimens for tensile test and bending test were 3D printed according to the Chinese testing standards of GB/T 1040.2-2006 (total length = 75 mm, width = 10 mm, and thickness = 2 mm) and GB/T 9341-2008 (total length = 64 mm, width = 10 mm, and thickness = 3.2 mm), respectively.

The mechanical properties were tested by universal testing machine (CTM8010, Xieqiang Instrument Manufacturing (Shanghai) Co., Ltd.). The test rate was 1 mm/min for both tests, and the gauge length was 30 mm for tensile test and 25 mm for bending test, respectively. Five samples were tested for statistics.

SEM photographs were taken by Apreo 2C (Thermo Fisher Scientific Co.) at the magnification of 200, 2000, and 5000.

Differential scanning calorimetry (DSC) was recorded by DSC1 (Mettler Toledo Instrument Co.) with a heating and cooling rate of 10°C/min in N_2.

3. Results and Discussion

In this study, 3 most widely used single-use plastics for packaging, i.e., PP, PE, and PET, are blended in a twin-screw extruder and then are drawn out to obtain feeding filaments for FDM. The filaments are 3D printed into SUPAs, and the mechanical properties, micromorphology, and thermal properties of the SUPAs are analyzed. This program is summarized in Figure 1.

3.1. Mechanical Properties

3.1.1. Effect of Blending Temperature. The three plastics have respective melting temperatures (T_m) with obvious difference (126-136°C for PE, 164-170°C for PP, and 250-255°C for PET). Therefore, they are processed at different temperature ranges, respectively. Choosing a suitable process temperature for the blend is the primary task. The overall composition of the single-use plastics for package is about 21 wt% PP, 36 wt% PE, and 10 wt% PET [2]. Therefore, a similar formula of $PP_{34}PE_{51}PET_{13}$ with 2 wt% PP-g-MAH (see Table 1) is first used to test the appropriate processing temperature. The processing temperature starts with 245°C, a little lower than the T_m of PET. Figure 2(a) shows the tensile strength of the specimens gradually increases with the increase of blending temperature from 245°C to 275°C. Taking the deviation in consideration, the tensile moduli are in a similar range. Furthermore, the flexural moduli and flexural strength exhibit slight increase with the increase of blending temperature (Figure 2(b)). In general, increasing blending temperature can promote the compatibility of the three plastics. However, the extruded filaments were obviously dark and black when the blending temperature was higher than 275°C, indicating obvious thermal decomposition during the blending process. Therefore, a temperature of 275°C was finally chosen as the processing temperature for the SUPAs.

Table 1: Formulation of the tested composites (unit: g).

Sample name	PE	PP	PET	PP-g-MAH	OMMT	Remark
$PP_{55}PE_{23}PET_{20}$	5.50	2.30	2.00	0.20	0	PP/PE = 70/30
$PP_{47}PE_{31}PET_{20}$	4.70	3.10	2.00	0.20	0	PP/PE = 60/40
$PP_{39}PE_{39}PET_{20}$	3.90	3.90	2.00	0.20	0	PP/PE = 50/50
$PP_{31}PE_{47}PET_{20}$	3.10	4.70	2.00	0.20	0	PP/PE = 40/60
PP-g-MAH1	3.20	4.70	2.00	0.10	0	PP/PE = 40/60
PP-g-MAH2	3.10	4.70	2.00	0.20	0	PP/PE = 40/60
PP-g-MAH3	3.10	4.60	2.00	0.30	0	PP/PE = 40/60
PP-g-MAH5	3.00	4.50	2.00	0.50	0	PP/PE = 40/60
OMMT0	3.10	4.70	2.00	0.20	0	PP/PE = 40/60
OMMT1	3.10	4.70	2.00	0.20	0.10	PP/PE = 40/60
OMMT2	3.10	4.70	2.00	0.20	0.20	PP/PE = 40/60
OMMT3	3.10	4.70	2.00	0.20	0.30	PP/PE = 40/60

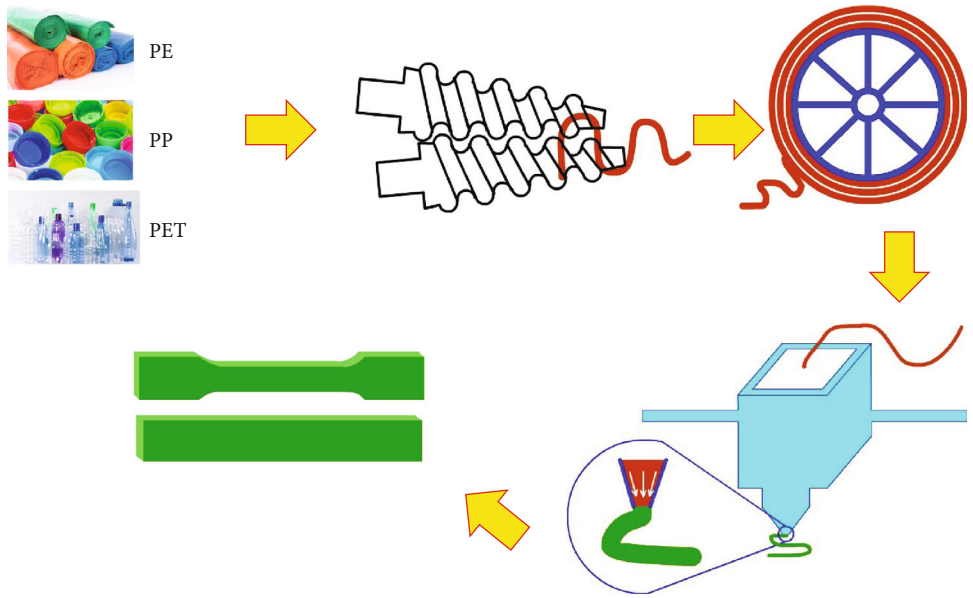

Figure 1: The process of 3D printing SUPA.

3.1.2. Effect of PET. PE and PP are POs with natural affinity. In spite of this, their differences in the molecular structure still affect the formation of crystalline zone, which therefore leads to the deterioration of mechanical properties. For instance, Strapasson et al. found that when PE and PP were mixed in the ratio of 50/50, the mechanical properties of the polymer alloy were the worst [36]. In contrast, the PET chain formed by polycondensation contains obvious polar repeating units, which is basically different from the POs. Therefore, it is always a research difficulty and highlight to well blend POs and PET [37]. In this section, the PET content is adjusted to investigate the mechanical properties of 3D-printed SUPA specimens. Based on the formula of PE 36 wt% and PP 21 wt%, the content of PET is increased from 10 to 30 wt% (Table 1), and the processing temperature is set at 275°C. In Figure 3(a), the tensile strength reaches the highest value when the PET content is 20 wt%. However, the tensile modulus shows high dispersion and the flexural strength and flexural modulus show a slight decrease for the SUPA with 20 wt% PET. These results imply an optimal formula and also no significant incompatibility for the SUPA samples which prepared according to the procedure in this work. Furthermore, Figure 3(b) shows that with increase PET content, the flexural strength and flexural modulus of the SUPA slightly decrease from 10 wt% to 20 wt% and finally increase at 30 wt% PET. PET forms fiber easier than PO companion during processing, which has been utilized [38]. It is speculated that these results are due to the primary fibrosis of PET macromolecules during the preparation of the filaments by drawing out the SUPA melt

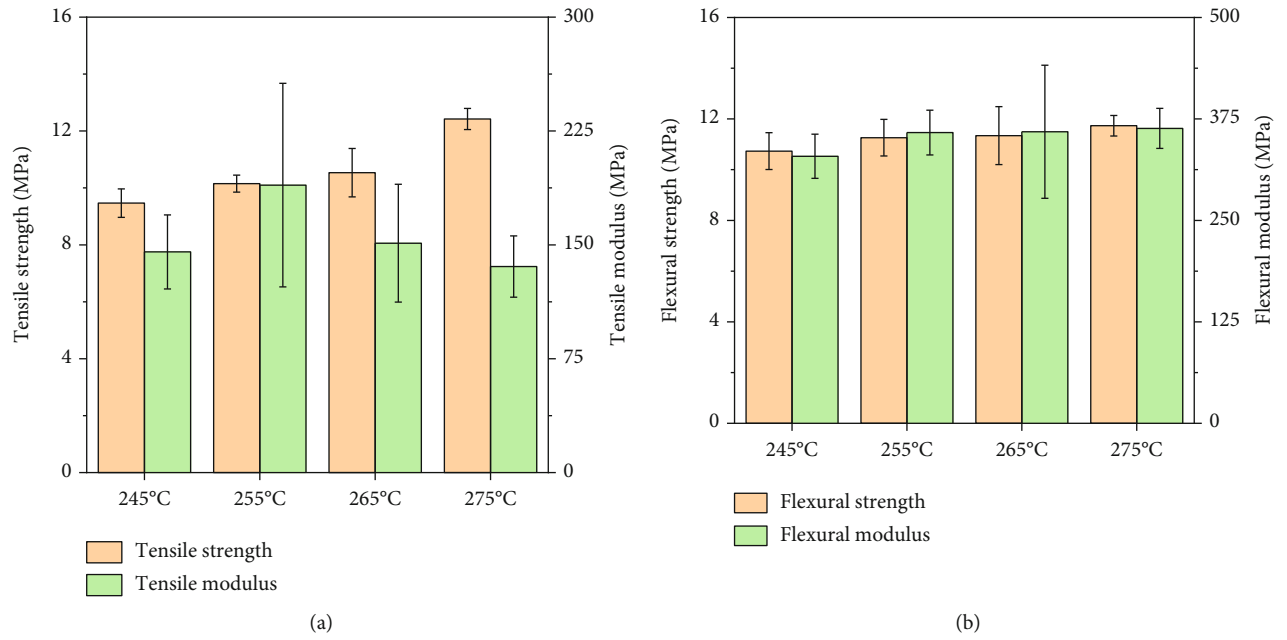

Figure 2: (a) Tensile strengths and tensile modulus of 3D-printed $PP_{34}PE_{51}PET_{13}$ (with 2 wt% PP-g-MAH) specimens and (b) its flexural strengths and flexural modulus at different blending temperatures.

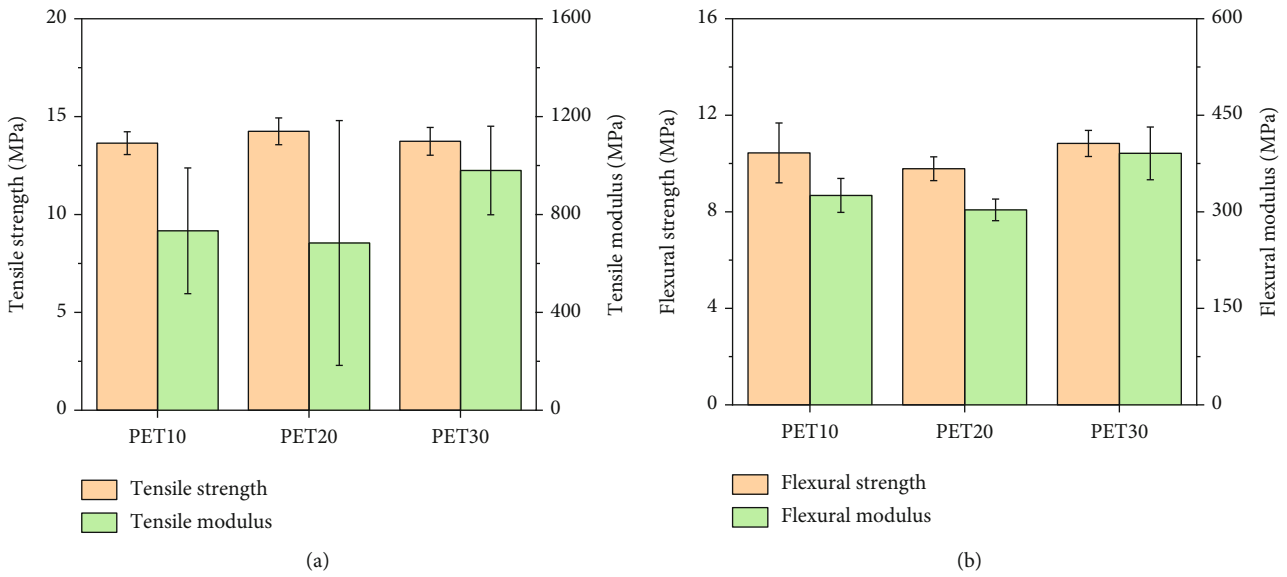

Figure 3: (a) The tensile strength and tensile modulus and (b) the flexural strength and flexural modulus of SUPAs with different PET contents.

and a secondary fibrosis at the nozzle of 3D printing. These oriented PET formed *in situ* and strengthened the SUPA.

3.1.3. Effect of Content Ratio of the POs. For PO blends, Şirin et al.'s results showed that the tensile strength continuously decreased with increasing PE content in the PO blends with peroxide [39]. Na et al. reported linear decreasing trends of tensile strength for PE in the PP matrix and PP in the PE matrix, and the minimum was obtained with PP/PE = 1 : 1 [13]. What will happen to the mechanical properties of SUPA when the ratio between the POs changes with PET in it? To the best of our knowledge, related result has not been reported. In this part, the content of PET was fixed at 20 wt% and the ratio of PP to PE was changed (see Table 1). Notably, the abovementioned trends are not clearly shown in Figure 4. When the PP/PE = 60/40 or 40/60, the alloy specimens have higher tensile strength. When PP/PE = 60/40, the tensile modulus exhibits the highest average value also with the broadest error bar. For the bending properties, the flexural modulus and strength of the SUPA samples show a 'smile' trend starting with PP/PE = 70/30 and ending with 40/60. Therefore, there are some advantageous

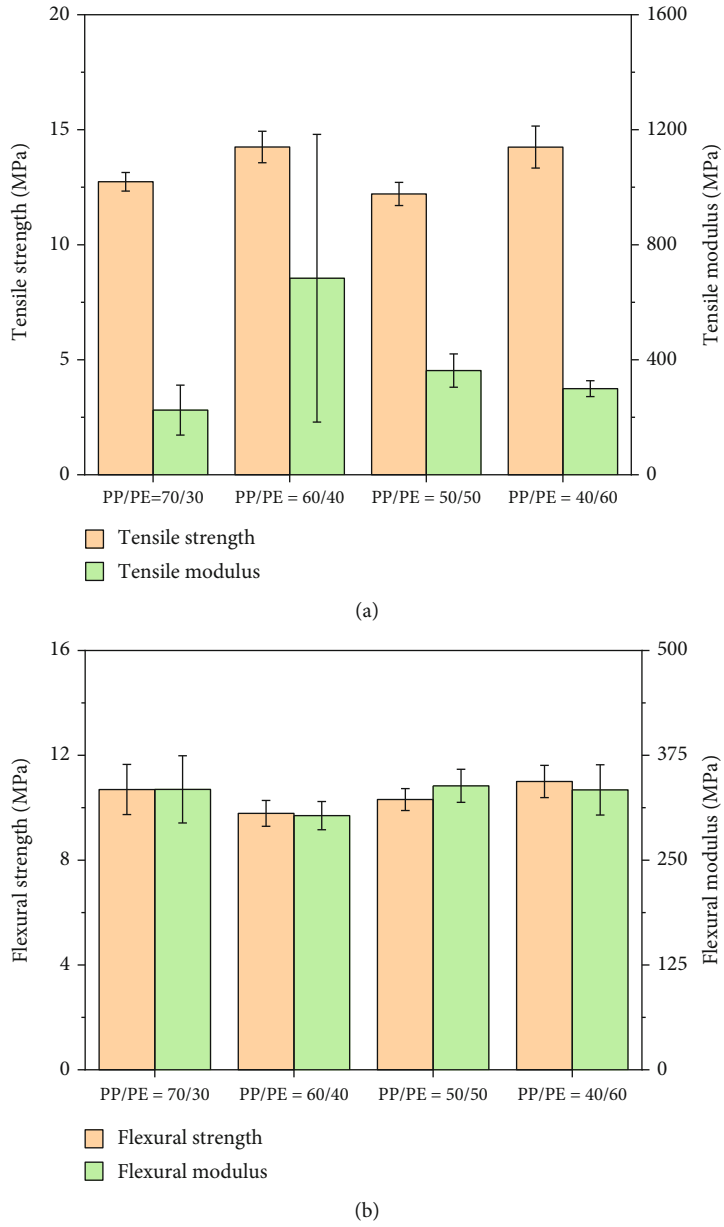

Figure 4: (a) The tensile strength and tensile modulus and (b) the flexural strength and flexural modulus of SUPAs with different content ratios of PP/PE.

ratios between POs in the SUPAs herein to achieve better mechanical performances. Based on the performances of PP/PE = 60/40 and 40/60 samples, they are adopted for the subsequent studies.

3.1.4. Effect of the Compatibilizer. In the SUPAs, the polyolefins and the polyester are difficult to compatible. If molecules that are compatible with both types of macromolecules are added as compatibilizers, the aggregation region of different phases will be effectively reduced and the molecular compatibility will be increased [17]. In this study, reactive compatibilizer of PP-g-MAH is used, whose main chain has affinity with POs and the side groups can react with PET to obtain grafting chain. Figure 5(a) shows that increasing PP-g-MAH from 1 wt% to 2 wt%, all of the tested mechanical properties increase, which proves improved interaction and adhesion between the POs and PET plastics and results in better stress transfer inside. However, when the content of compatibilizer further increases, the mechanical strength in the tensile and bending tests decreases. The reason could be attributed to the elastomeric property of the compatibilizer, which deteriorates the mechanical properties of the tested samples [15, 16].

The results of flexural strength and flexural modulus of SUPAs are shown in Figure 5(b). When the amount of compatibilizer increases, the flexural strength of the material first increases and then decreases with an obvious downward trend. When the content of PP-g-MAH is 2 wt%, the resulting SUPA has the highest flexural strength

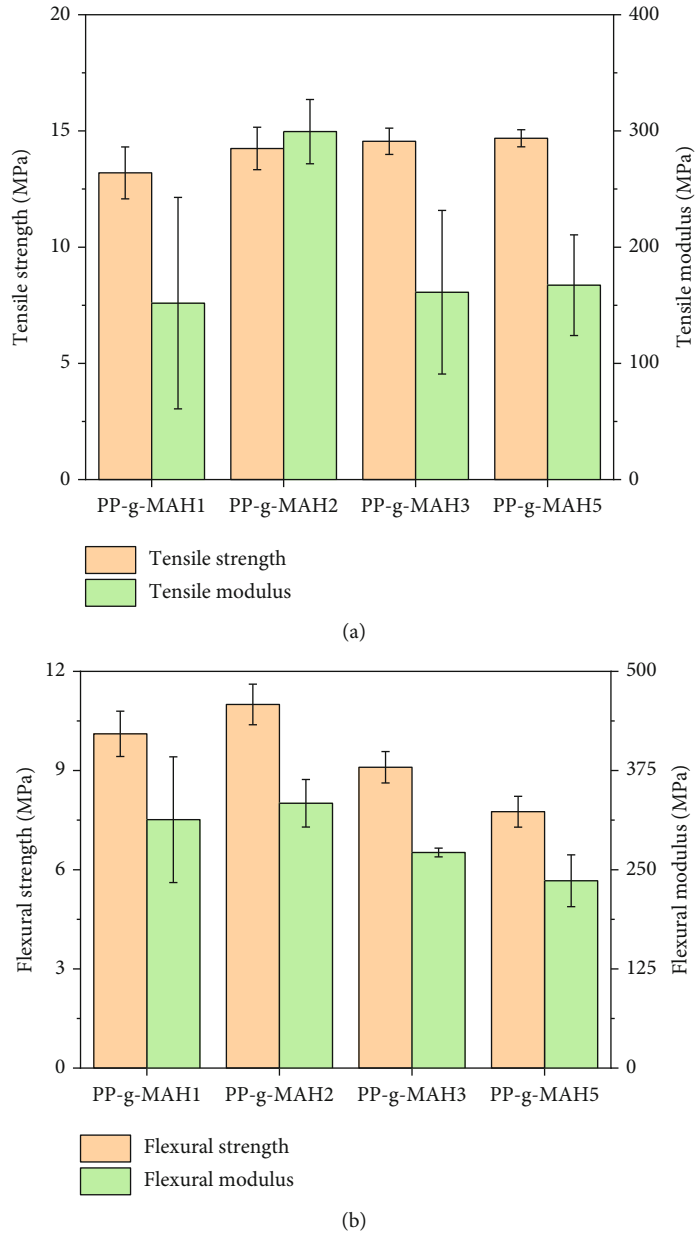

Figure 5: (a) The tensile strength and tensile modulus and (b) the flexural strength and flexural modulus of SUPAs with different PP-g-MAH contents.

(14.25 ± 0.91 MPa) and flexural modulus (299.45 ± 27.65 MPa) among all the tested samples in this section. The reason for this result can be attributed to the good compatibilization plus dispersion of fibrous PET.

3.1.5. Effect of the NC. Using NC to increase the mechanical properties of composites is well established [37, 40, 41]. To increase the compatibility between a NC and the plastic matrix, organic modification is always adopted. Based on the formula of 2 wt% PP-g-MAH, we further prepared SUPAs with OMMT. Figure 6 shows the results of tensile and bending tests. The results show that the addition of OMMT significantly enhances the mechanical properties of the tested composites. Comparing with the samples without OMMT (OMMT0), the tensile modulus of OMMT2 is nearly doubled. Furthermore, the flexural strength and flexural modulus of OMMT2 increase by 44 wt% and 62 wt%, respectively, comparing with OMMT0. The results imply that the organically modified MMT could improve the compatibility of POs and PET by interface fusion. Furthermore, the inherent high modulus of NC could also contribute the mechanical properties of the composites. Nonetheless, overload of NC may not continuously increase the mechanical performances. The highest tensile strength was obtained with OMMT3, but the highest flexural strength was obtained with OMMT2. The reason could be attributed to some agglomerate of the OMMT, which created nonuniform stress regions [42].

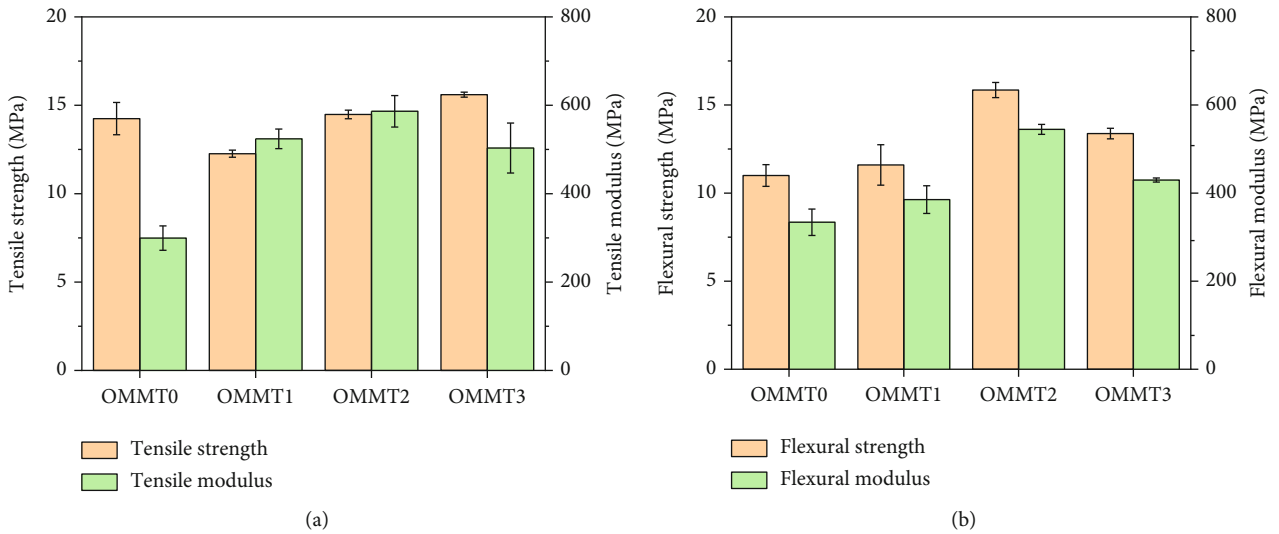

Figure 6: (a) The tensile strength and tensile modulus and (b) the flexural strength and flexural modulus of SUPAs with different OMMT contents.

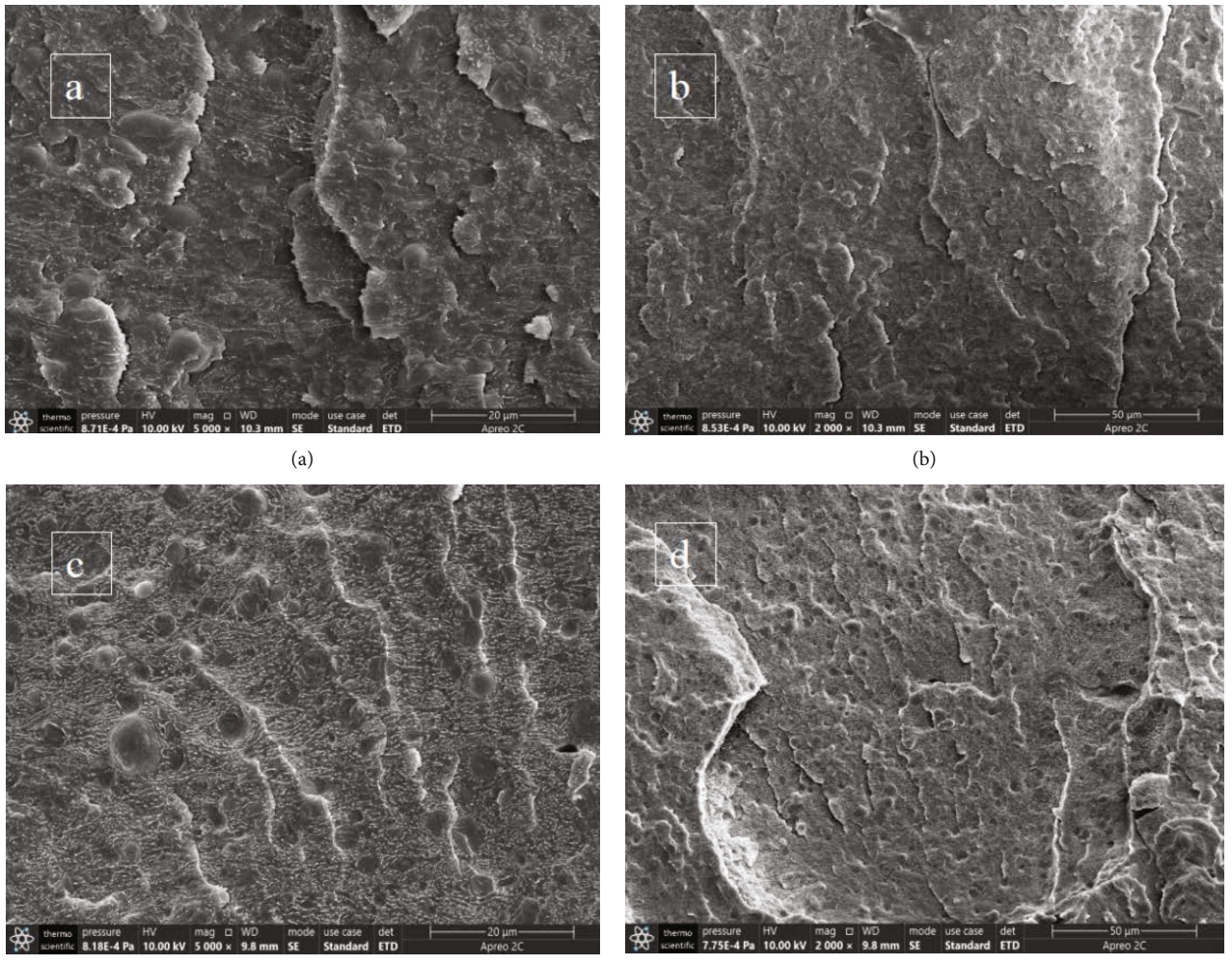

Figure 7: SEM photographs of $PP_{47}PE_{31}PET_{20}$ at the magnification of 5000 (a) and 2000 (b) and $PP_{31}PE_{47}PET_{20}$ at the magnification of 5000 (c) and 2000 (d).

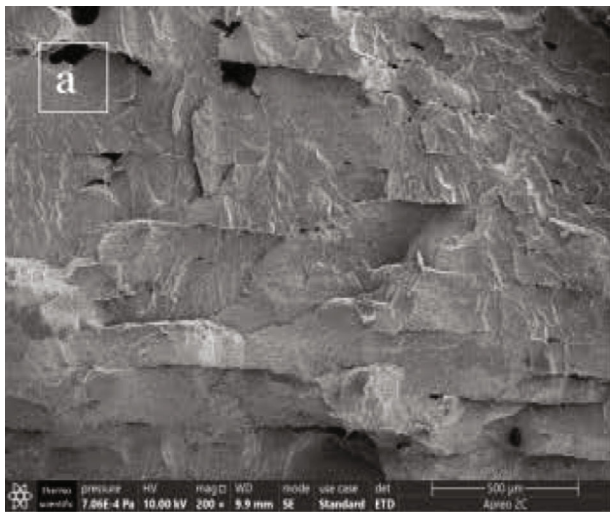

(a)

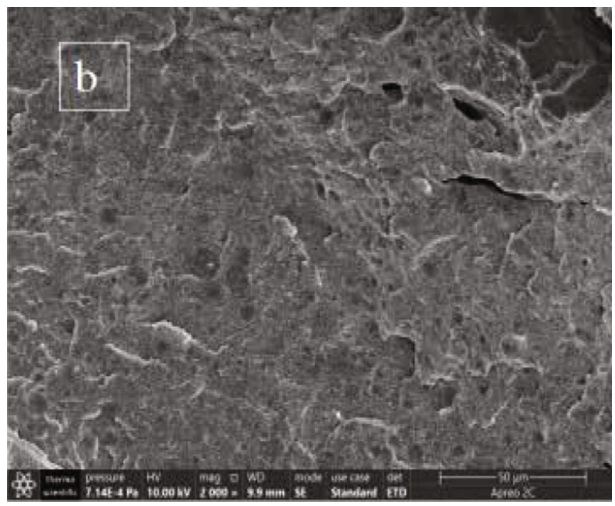

(b)

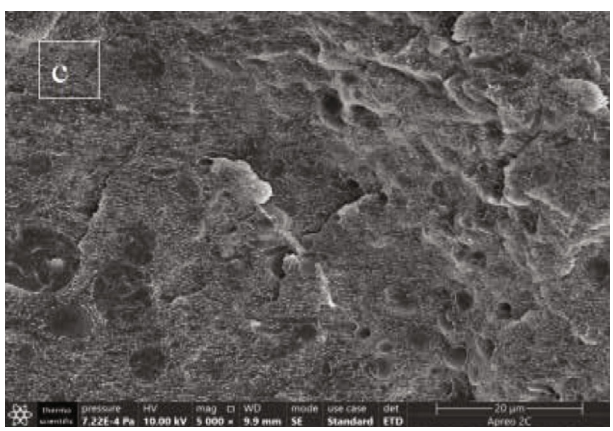

(c)

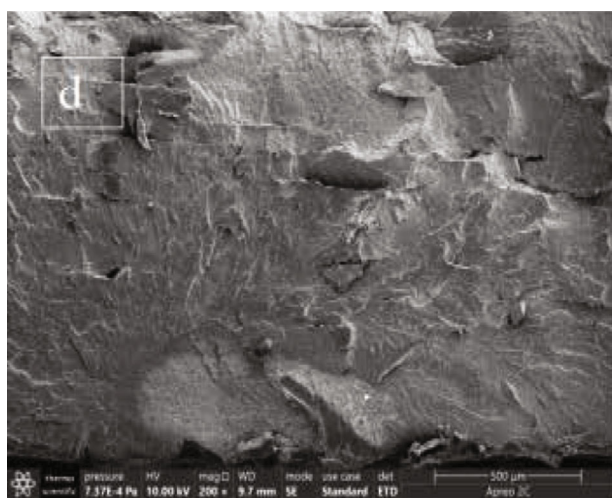

(d)

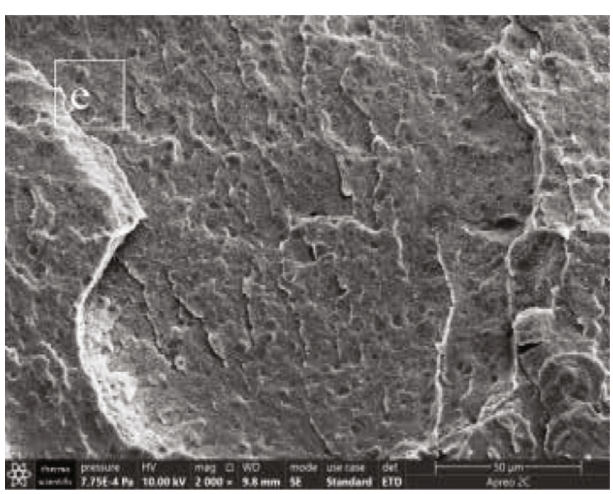

(e)

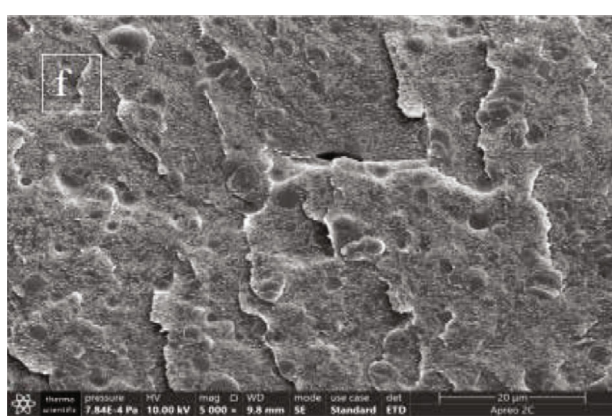

(f)

Figure 8: Continued.

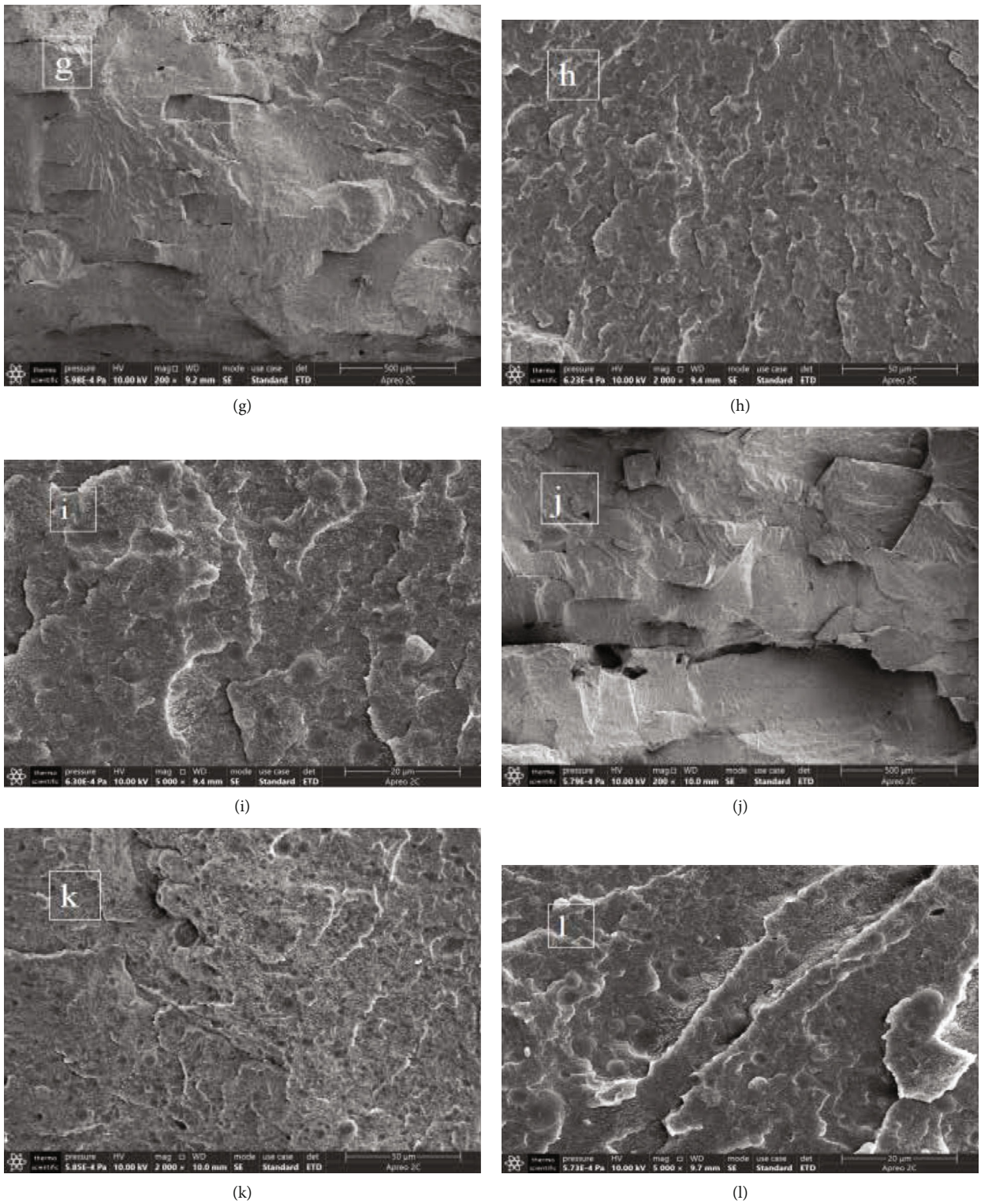

(g) (h)

(i) (j)

(k) (l)

Figure 8: SEM photographs of PP-g-MAH1 at the magnification of 200 (a), 2000 (b), and 5000 (c); PP-g-MAH2 at the magnification of 200 (d), 2000 (e), and 5000 (f); PP-g-MAH3 at the magnification of 200 (g), 2000 (h), and 5000 (i); and PP-g-MAH5 at the magnification of 200 (j), 2000 (k), and 5000 (l).

3.2. Morphology Analysis of Compatibilized SUPAs. SEM is used to scan the cross section of 3D-printed specimens to study the potential fibrosis of PET. Figure 7 shows the SEM photographs of $PP_{47}PE_{31}PET_{20}$ (PP/PE = 60/40) and $PP_{31}PE_{47}PET_{20}$ (PP/PE = 40/60). If no compatibilization is applied, obvious 'islands' will appear in the blend of PP and PET [15, 16]. Comparing the SEM images of the two components at the same magnification, morphology of

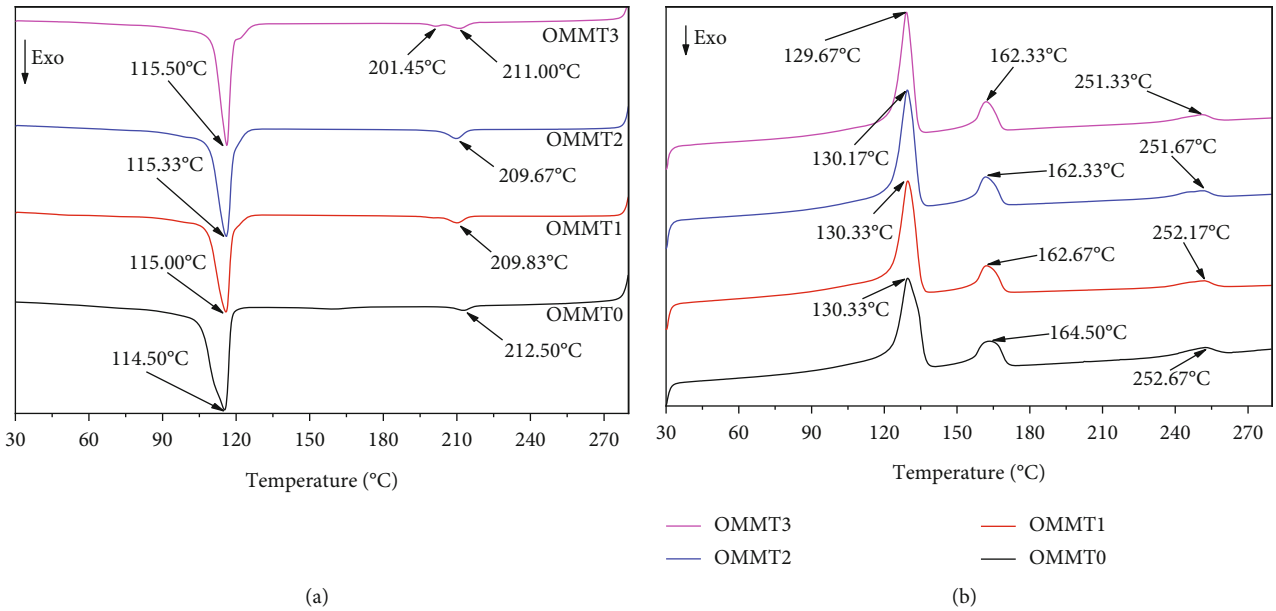

Figure 9: (a) The DSC curves of 3D-printed OMMT0, OMMT1, OMMT2, and OMMT3 composite specimens. (b) Melting temperature curves of 3D-printed OMMT0, OMMT1, OMMT2, and OMMT3 composites.

$PP_{47}PE_{31}PET_{20}$ is relatively smooth, and the phase boundary between the 3 components is unclear. This result may be based on the good compatibilization effect of PP-g-MAH in the SUPA.

In comparison, the phase boundary in the sample of $PP_{31}PE_{47}PET_{20}$ can be distinguished, which confirms the *in situ* fibrosis of PET during drawing filaments. In addition, the nozzle of 3D printing is speculated to play a role of promoting orientation of PET, too. The PET fibers formed in these actions bear stress when it subjected to external forces and therefore enhance the mechanical properties of the alloy.

Figure 8 further exhibits the SEM photographs of 3D-printed composite specimens with different compatibilizer contents. At the magnification of 200 times, the interlayer fusion in the printing specimens is good, which verifies the high-quality process of 3D printing. Comparing with the photographs with higher magnifications, it can be found that the fiber area, i.e., PET, first decreases and then increases. In addition, both the particle-like area and the PET area of 2 wt% PP-g-MAH sample are the smallest among all the tested samples, which corresponds to its superior mechanical properties. However, the particle area in the PP-g-MAH5 increases again, which is not because the compatibility between polymers becomes worse, but because the compatibilizer itself forms agglomerates with their essential affinity. This behavior explains why the bending properties of the SUPAs increase first and then decrease with the increase of the compatibilizer.

3.3. Thermal Behaviors of the SUPAs. Since the use of compatibilizer and OMMT greatly improved the mechanical properties of 3D-printed SUPA, DSC tests were used to study the crystallization behavior of the composites with both PP-g-MAH and OMMT. From the DSC results (Figure 9(a)), the bigger peak of crystallization moves to the higher temperature, which is due to the OMMT can enhance the compatibility between PP, PE, and PET, reduce the free energy of nucleation interface, and promote heterogeneous nucleation [43, 44]. There is a smaller peak of crystallization in each testing sample, which corresponds to the incompatible PET particles. In comparison, the DSC curve of OMMT3 has 2 small peaks of crystallization, which are partially overlapped. This result makes the crystallization peak of PET shift to the right and the other small peaks shift to the left. The small peaks shifting left are aggregates of OMMTs, which is consistent with the results of mechanical tests. The addition of PP-g-MAH could increase the compatibility between POs and PET, however, which delays the crystallization. The decrease of the crystallization rate and the increase of crystallization temperature can therefore maintain the high thermal deformation temperature and mechanical properties of the material, which also corresponds to the result of obvious improvement of the mechanical properties of the SUPA containing OMMT [37, 40, 41]. In addition, one can easily find PE (T_m at 126-136°C), PP (T_m at 164-170°C), and PET (T_m at 250-255°C) in the melting temperature curves (Figure 9(b)). After adding OMMT into the SUPA, all the melting peaks of the 3 plastics move towards low temperature. In addition, increase of the amount of OMMT reinforces this trend. This result indicates that OMMT has an impact on the crystallinity of the plastics [45–47]. The main reason could be reduced repulsive force and increased compatibility between POs and PET through OMMT.

4. Conclusion

In this study, plastic alloys based on disposable packaging plastics are prepared by melt blending and wire drawing first, and then, standard mechanical test specimens are 3D printed by fused deposition modeling. In addition, a reactive

compatibilizer of PP-g-MAH and/or organically modified montmorillonite are used to improve the compatibility and mechanical strength. SEM and DSC technologies are used for the micromorphology and crystallinity studies.

Due to the difference in melting points of the disposable packaging plastics, there is optimum processing temperature for the SUPA. The results show that the SUPA has the best mechanical properties when processed below the thermal degradation temperature of the polyolefin. When the content of PET around the composition of disposable packaging plastics increased, the tensile and bending properties of 3D-printed specimens tend to improve, which could be attributed to the primary microfiber pulling effect during collecting printing filaments and the secondary microfiber pulling effect in the printing nozzles. Furthermore, the proportion of polyolefins has a significant effect on the mechanical properties of the alloy. The specimen of PP/PE = 40/60 with 20 wt% PET has the highest tensile strength and tensile modulus. The use of PP-g-MAH can increase the compatibility of the three plastics, thus improving the mechanical strength of the specimens. However, due to the elastomer and aggregation of compatibilizers, excessive compatibilizers will deteriorate the mechanical performance. The organically modified montmorillonite could well disperse at the phase interface of the plastics, which contributes to the compatibilization and reinforcement. However, the agglomerate of excessive nanoclay will form stress concentration areas and also deteriorate mechanical properties. Finally, due to the function of compatibilizer and nanoclay will be affected by redundancy, the potential primary fibrosis while collecting the feeding filaments and the secondary fibrosis at the nozzle of 3D printing might be responsible for the variation of the mechanical performances.

Data Availability

Data will be available upon necessary request.

Conflicts of Interest

The authors declare that they have no conflicts of interest.

Acknowledgments

The authors appreciate the financial support from the Natural Science Foundation of Sichuan Province (2022NSFSC0391), National Natural Science Foundation of China (Grant 51603130), and 'Young Scholars' support plan of Xihua University.

References

[1] Plastics Europe, *Plastics – the facts 2019: an analysis of European plastics production, demand and waste data*, Plastics Europe, 2019.

[2] R. Geyer, J. R. Jambeck, and K. L. Law, "Production, use, and fate of all plastics ever made," *Science Advances*, vol. 3, no. 7, p. e1700782, 2017.

[3] I. A. Ignatyev, W. Thielemans, and B. V. Beke, "Recycling of polymers: a review," *ChemSusChem*, vol. 2014, pp. 1579–1593, 2014.

[4] Y. Chen, A. K. Awasthi, F. Wei, Q. Tan, and J. Li, "Single-use plastics: production, usage, disposal, and adverse impacts," *Science of the Total Environment*, vol. 752, 2021.

[5] K. Saito, C. Jehanno, L. Meabe et al., "From plastic waste to polymer electrolytes for batteries through chemical upcycling of polycarbonate," *Journal of Materials Chemistry A*, vol. 8, no. 28, pp. 13921–13926, 2020.

[6] M. Haussler, M. Eck, D. Rothauer, and S. Mecking, "Closed-loop recycling of polyethylene-like materials," *Nature*, vol. 590, no. 7846, pp. 423–427, 2021.

[7] K. Lewandowski, K. Skorczewska, K. Piszczek, and W. Urbaniak, "Recycled glass fibres from wind turbines as a filler for poly(vinyl chloride)," *Advances in Polymer Technology*, vol. 2019, Article ID 8960503, 11 pages, 2019.

[8] M. Xanthos, "Recycling of the #5 polymer (vol 337, pg 700, 2012)," *Science*, vol. 338, no. 6107, p. 604, 2012.

[9] L. Bohn, "Incompatibility and phase formation in solid polymer mixures and graft and block copolymers," *Rubber Chemistry and Technology*, vol. 1968, pp. 495–513, 1968.

[10] G. Zhang, Q. Fu, K. Z. Shen, L. Jian, and Y. Wang, "Studies on blends of high-density polyethylene and polypropylene produced by oscillating shear stress field," *Journal of Applied Polymer Science*, vol. 86, no. 1, pp. 58–63, 2002.

[11] A. Dhoble, B. Kulshreshtha, S. Ramaswami, and D. A. Zumbrunnen, "Mechanical properties of PP-LDPE blends with novel morphologies produced with a continuous chaotic advection blender," *Polymer*, vol. 46, no. 7, pp. 2244–2256, 2005.

[12] B. Na, K. Wang, P. Zhao et al., "Epitaxy growth and directed crystallization of high-density polyethylene in the oriented blends with isotactic polypropylene," *Polymer*, vol. 46, no. 14, pp. 5258–5267, 2005.

[13] B. Na, K. Wang, Q. Zhang, R. N. Du, and Q. Fu, "Tensile properties in the oriented blends of high-density polyethylene and isotactic polypropylene obtained by dynamic packing injection molding," *Polymer*, vol. 46, no. 9, pp. 3190–3198, 2005.

[14] I. Charfeddine, J. C. Majeste, C. Carrot, and O. Lhost, "Predicting the Young's modulus and the impact strength of immiscible polyolefin blends," *Polymer*, vol. 204, p. 122795, 2020.

[15] H. Inoya, Y. W. Leong, W. Klinklai, Y. Takai, and H. Hamada, "Compatibilization of recycled poly(ethylene terephthalate) and polypropylene blends: effect of compatibilization on blend toughness, dispersion of minor phase, and thermal stability," *Journal of Applied Polymer Science*, vol. 124, no. 6, pp. 5260–5269, 2012.

[16] H. Inoya, Y. W. Leong, W. Klinklai, S. Thumsorn, Y. Makata, and H. Hamada, "Compatibilization of recycled poly(ethylene terephthalate) and polypropylene blends: effect of polypropylene molecular weight on homogeneity and compatibility," *Journal of Applied Polymer Science*, vol. 124, no. 5, pp. 3947–3955, 2012.

[17] J. L. Self, A. J. Zervoudakis, X. Peng, W. R. Lenart, C. W. Macosko, and C. J. Ellison, "Linear, graft, and beyond: multiblock copolymers as next-generation compatibilizers," *JACS Au*, vol. 2, no. 2, pp. 310–321, 2022.

[18] F. I. Seyni and B. P. Grady, "Janus particles as immiscible polymer blend compatibilizers: a review," *Colloid & Polymer Science*, vol. 299, no. 4, pp. 585–593, 2021.

[19] M. Huang and A. K. Schlarb, "Polypropylene/poly(ethylene terephthalate) microfibrillar reinforced composites manufactured by fused filament fabrication," *Journal of Applied Polymer Science*, vol. 138, no. 23, p. 50557, 2021.

[20] S. Luo, J. Sun, A. Huang, T. Zhang, L. Wei, and S. Qin, "In situ fibrillation of isotactic polypropylene in ethylene-vinyl acetate: toward enhanced rheological and mechanical properties," *Journal of Applied Polymer Science*, vol. 136, no. 21, p. 47557, 2019.

[21] S. Kordjazi, Z. Kordjazi, and N. G. Ebrahimi, "The effect of different compatibilisers on the morphology and rheological properties of PP/PET polymer blends," *Plastics, Rubber and Composites*, vol. 51, no. 5, pp. 250–258, 2022.

[22] I. Fortelny and J. Juza, "The effects of copolymer compatibilizers on the phase structure evolution in polymer blends-a review," *Materials*, vol. 14, no. 24, p. 7786, 2021.

[23] S. B. Aziz, M. H. Hamsan, M. F. Z. Kadir, and H. J. Woo, "Design of polymer blends based on chitosan:POZ with improved dielectric constant for application in polymer electrolytes and flexible electronics," *Advances in Polymer Technology*, vol. 2020, Article ID 8586136, 10 pages, 2020.

[24] K. T. Lau, C. Gu, and D. Hui, "A critical review on nanotube and nanotube/nanoclay related polymer composite materials," *Composites Part B: Engineering*, vol. 37, no. 6, pp. 425–436, 2006.

[25] R. S. Chen, S. Ahmad, and S. Gan, "Characterization of recycled thermoplastics-based nanocomposites: polymer-clay compatibility, blending procedure, processing condition, and clay content effects," *Composites Part B: Engineering*, vol. 131, pp. 91–99, 2017.

[26] M. Ahmadlouydarab, M. Chamkouri, and H. Chamkouri, "Compatibilization of immiscible polymer blends (R-PET/PP) by adding PP-g-MA as compatibilizer: analysis of phase morphology and mechanical properties," *Polymer Bulletin*, vol. 77, no. 11, pp. 5753–5766, 2020.

[27] K. Jayanarayanan, S. Thomas, and K. Joseph, "In situ microfibrillar blends and composites of polypropylene and poly (ethylene terephthalate): morphology and thermal properties," *Journal of Polymer Research*, vol. 2011, pp. 1–11, 2011.

[28] N. E. Zander, M. Gillan, Z. Burckhard, and F. Gardea, "Recycled polypropylene blends as novel 3D printing materials," *Additive Manufacturing*, vol. 25, pp. 122–130, 2019.

[29] T. D. Ngo, A. Kashani, G. Imbalzano, K. T. Q. Nguyen, and D. Hui, "Additive manufacturing (3D printing): a review of materials, methods, applications and challenges," *Composites Part B: Engineering*, vol. 143, pp. 172–196, 2018.

[30] F. M. Mwania, M. Maringa, and K. van der Walt, "A review of methods used to reduce the effects of high temperature associated with polyamide 12 and polypropylene laser sintering," *Advances in Polymer Technology*, vol. 2020, Article ID 9497158, 11 pages, 2020.

[31] O. A. Mohamed, S. H. Masood, and J. L. Bhowmik, "Optimization of fused deposition modeling process parameters: a review of current research and future prospects," *Advanced Manufacturing*, vol. 3, no. 1, pp. 42–53, 2015.

[32] S. Coppola, G. Nasti, V. Vespini, and P. Ferraro, "Layered 3D printing by tethered pyro-electrospinning," *Advances in Polymer Technology*, vol. 2020, Article ID 1252960, 9 pages, 2020.

[33] B. N. Turner, R. Strong, and S. A. Gold, "A review of melt extrusion additive manufacturing processes: I. Process design and modeling," *Rapid Prototyping Journal*, vol. 20, no. 3, pp. 192–204, 2014.

[34] G. Spinelli, P. Lamberti, V. Tucci et al., "Nanocarbon/poly(lactic) acid for 3D printing: effect of fillers content on electromagnetic and thermal properties," *Materials*, vol. 12, no. 15, 2019.

[35] B. N. Turner and S. A. Gold, "A review of melt extrusion additive manufacturing processes: II. Materials, dimensional accuracy, and surface roughness," *Rapid Prototyping Journal*, vol. 21, no. 3, pp. 250–261, 2015.

[36] R. Strapasson, S. C. Amico, M. F. R. Pereira, and T. H. D. Syclenstricker, "Tensile and impact behavior of polypropylene/low density polyethylene blends," *Polymer Testing*, vol. 24, no. 4, pp. 468–473, 2005.

[37] A. K. Singh, R. Bedi, and B. S. Kaith, "Composite materials based on recycled polyethylene terephthalate and their properties - a comprehensive review," *Composites Part B: Engineering*, vol. 219, p. 108928, 2021.

[38] K. Friedrich, M. Evstatiev, S. Fakirov, O. Evstatiev, M. Ishii, and M. Harrass, "Microfibrillar reinforced composites from PET/PP blends: processing, morphology and mechanical properties," *Composites Science and Technology*, vol. 65, no. 1, pp. 107–116, 2005.

[39] K. Sirin, F. Dogan, M. Canli, and M. Yavuz, "Mechanical properties of polypropylene (PP) + high-density polyethylene (HDPE) binary blends: non-isothermal degradation kinetics of PP + HDPE (80/20) blends," *Polymers for Advanced Technologies*, vol. 24, pp. 715–722, 2013.

[40] Y. J. Li, W. Y. Dong, H. T. Wang et al., "New pathways to high-performance immiscible polymer blends by reactive compatibilization: comb-like molecular, nanomicellar, and nanoparticulate strategies," *Science*, vol. 360, pp. 17-18, 2018.

[41] L. A. Goettler, K. Y. Lee, and H. Thakkar, "Layered silicate reinforced polymer nanocomposites: development and applications," *Polymer Reviews*, vol. 47, no. 2, pp. 291–317, 2007.

[42] Y. Chen, Z. Guo, and Z. Fang, "Relationship between the distribution of organo-montmorillonite and the flammability of flame retardant polypropylene," *Polymer Engineering and Science*, vol. 52, no. 2, pp. 390–398, 2012.

[43] C. Ding, D. M. Jia, H. He, B. C. Guo, and H. Q. Hong, "How organo-montmorillonite truly affects the structure and properties of polypropylene," *Polymer Testing*, vol. 24, no. 1, pp. 94–100, 2005.

[44] S. S. Ray and M. Bousmina, "Compatibilization efficiency of organoclay in an immiscible polycarbonate/poly(methyl methacrylate) blend," *Macromolecular Rapid Communications*, vol. 26, no. 6, pp. 450–455, 2005.

[45] W. S. Chow and S. K. Lok, "Thermal properties of poly(lactic acid)/organo-montmorillonite nanocomposites," *Journal of Thermal Analysis and Calorimetry*, vol. 95, no. 2, pp. 627–632, 2009.

[46] S. S. Ray and M. Bousmina, "Poly(butylene sucinate- *co* -adipate)/montmorillonite nanocomposites: effect of organic modifier miscibility on structure, properties, and viscoelasticity," *Polymer*, vol. 46, no. 26, pp. 12430–12439, 2005.

[47] X. Q. Zhang, M. S. Yang, Y. Zhao et al., "Polypropylene/montmorillonite composites and their application in hybrid fiber preparation by melt-spinning," *Journal of Applied Polymer Science*, vol. 92, no. 1, pp. 552–558, 2004.